Neurotherapeutics 21 (2024) e00350

Contents lists available at ScienceDirect

Neurotherapeutics

journal homepage: www.sciencedirect.com/journal/neurotherapeutics

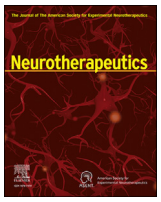

Original Article

Fosgonimeton attenuates amyloid-beta toxicity in preclinical models of Alzheimer's disease

Sherif M. Reda, Sharay E. Setti, Andrée-Anne Berthiaume, Wei Wu, Robert W. Taylor, Jewel L. Johnston, Liana R. Stein, Hans J. Moebius, Kevin J. Church *

Athira Pharma, Inc., 18706 North Creek Parkway, Suite 104, Bothell, WA, 98011, USA

ARTICLE INFO

Keywords:
Fosgonimeton
Alzheimer's disease
Hepatocyte growth factor (HGF)
Neurotrophic factor
Neuroprotection
Amyloid beta

ABSTRACT

Positive modulation of hepatocyte growth factor (HGF) signaling may represent a promising therapeutic strategy for Alzheimer's disease (AD) based on its multimodal neurotrophic, neuroprotective, and anti-inflammatory effects addressing the complex pathophysiology of neurodegeneration. Fosgonimeton is a small-molecule positive modulator of the HGF system that has demonstrated neurotrophic and pro-cognitive effects in preclinical models of dementia. Herein, we evaluate the neuroprotective potential of fosgonimeton, or its active metabolite, fosgo-AM, in amyloid-beta (Aβ)-driven preclinical models of AD, providing mechanistic insight into its mode of action. In primary rat cortical neurons challenged with Aβ ($Aβ_{1-42}$), fosgo-AM treatment significantly improved neuronal survival, protected neurite networks, and reduced tau hyperphosphorylation. Interrogation of intracellular events indicated that cortical neurons treated with fosgo-AM exhibited a significant decrease in mitochondrial oxidative stress and cytochrome *c* release. Following Aβ injury, fosgo-AM significantly enhanced activation of pro-survival effectors ERK and AKT, and reduced activity of GSK3β, one of the main kinases involved in tau hyperphosphorylation. Fosgo-AM also mitigated Aβ-induced deficits in Unc-like kinase 1 (ULK1) and Beclin-1, suggesting a potential effect on autophagy. Treatment with fosgo-AM protected cortical neurons from glutamate excitotoxicity, and such effects were abolished in the presence of an AKT or MEK/ERK inhibitor. In vivo, fosgonimeton administration led to functional improvement in an intracerebroventricular $Aβ_{25-35}$ rat model of AD, as it significantly rescued cognitive function in the passive avoidance test. Together, our data demonstrate the ability of fosgonimeton to counteract mechanisms of Aβ-induced toxicity. Fosgonimeton is currently in clinical trials for mild-to-moderate AD (NCT04488419; NCT04886063).

Introduction

Alzheimer's disease (AD) is a progressive and fatal neurodegenerative disorder that accounts for 60–80% of all dementia cases [1,2]. The major pathological hallmarks of AD are the extracellular deposition of amyloid-beta (Aβ) peptides in the form of plaques, and the intracellular accumulation of hyperphosphorylated tau (pTau) protein as neurofibrillary tangles. Aβ- and tau-induced cytotoxicity are key disease components underpinning the neuronal loss and synaptic dysfunction observed in the brains of people with AD and are therefore considered to be major drivers of neurodegeneration. In addition to this protein pathology, numerous ongoing cellular processes contribute to the progression of the disease, including oxidative stress, excitotoxicity [3], neuroinflammation [4,5], neurotransmission abnormalities [6,7], neurotrophic growth factor deficits [8,9], metabolic dysfunction [10,11], and cerebrovascular dysfunction [12].

One of the predominant theories regarding the etiology of AD is the amyloid cascade hypothesis, which posits that the abnormal deposition of Aβ aggregates is the initial cause of AD, and all other pathological changes follow this precipitating event [13]. Indeed, it has been reported that exposure to neurotoxic Aβ peptides can result in many of the observed components of AD, including excitotoxicity, neuroinflammation, oxidative stress, and heightened neurodegeneration [14–16]. Intracellular accumulation of Aβ can directly dysregulate several processes including, but not limited to, cellular respiration (via mitochondrial dysfunction and oxidative stress) [17–19], autophagy-lysosomal pathways [20,21], and kinase signaling [22–24]. Critically, the relationship between Aβ aggregation and ensuing disease pathology is bidirectional and cyclical, constituting a vicious cycle that promotes neuronal death and loss of neuronal network connectivity. For instance, the increased oxidative stress and neuroinflammation elicited by Aβ accumulation may, in turn, lead to the generation of more toxic

* Corresponding author.
E-mail address: kevin.church@athira.com (K.J. Church).

https://doi.org/10.1016/j.neurot.2024.e00350
Received 14 September 2023; Received in revised form 13 March 2024; Accepted 16 March 2024

protein aggregates which further compromise cellular functions. Thus, it is likely that regardless of whether the initial triggering events are driven by amyloid pathology or otherwise, by the time AD becomes symptomatic and diagnosed, the various secondary disease processes have become self-perpetuating and uncoupled from the initiating factors.

Based on the multifaceted and cyclical nature of AD pathophysiology, therapies targeting a single facet of the disease, such as protein pathology, may have natural limitations. For instance, some interventions that are effective at reducing Aβ protein load have demonstrated significant slowing of cognitive decline in early AD, but the magnitude of the effect is limited [25,26]. Primarily addressing protein pathology with little impact on the enormous pathological burden of ongoing secondary disease processes is one possible explanation for such outcomes [27] and suggests that additional interventions are needed. Specifically, therapeutic approaches targeting multiple disease components simultaneously, including the pathological mechanisms associated with Aβ protein aggregation, may prove beneficial. Neurotrophic factors are one possible therapeutic target for AD, based on the reported wide array of favorable effects on neurons and support cells induced by their signaling cascades [28–32]. In particular, hepatocyte growth factor (HGF) signaling via its singular receptor, MET, presents a novel opportunity for intervention, as HGF promotes a plethora of signaling cascades that regulate neurotrophic and neuroprotective processes [28,32–34]. Upon binding of HGF, the MET receptor undergoes dimerization and autophosphorylation, resulting in the activation of neurotrophic and pro-survival signaling pathways including phosphatidylinositol 3-kinase (PI3K)/AKT, extracellular signal-regulated kinase (ERK), and protein kinase C (PKC) pathways [32,33,35]. Consequently, activation of MET by HGF plays a significant role in promoting the development, maintenance, and repair of the nervous system [33]. Indeed, HGF signaling induces pro-survival and anti-apoptotic mechanisms [36], as well as modulation of neurotransmission [37]. With regard to AD pathology, clinical data have demonstrated a decrease in the expression of MET in the brains of people with AD [38]. Furthermore, reduced HGF/MET signaling has been implicated in synaptic pathology observed in an AD mouse model [39]. Therefore, correction of this deficit and enhancement of HGF/MET-induced neurotrophic and neuroprotective effects may present a novel therapeutic avenue for AD [28].

We have developed a series of brain-penetrant small molecule positive modulators of the neurotrophic HGF signaling system for the treatment of neurodegenerative conditions, including AD. One such molecule, fosgonimeton (or its active metabolite, fosgo-AM), has demonstrated neurotrophic, neuroprotective, and anti-inflammatory effects in vitro and in vivo (40). In the current study, we expand on these findings to assess the preclinical efficacy of fosgonimeton in the context of Aβ-driven models of AD. Specifically, we evaluate the neuroprotective effects of fosgo-AM in Aβ-challenged primary cortical neurons and present mechanistic insight into its mode of action. We then utilize intracerebroventricular (ICV) delivery of a neurotoxic $A\beta_{25-35}$ peptide fragment in rats to assess the ability of fosgonimeton to confer protection against cognitive deficits induced by Aβ pathology.

Methods

In vitro assays

Animals

The following experiments were carried out in accordance with the National Research Council Guide for the Care and Use of Laboratory Animals and followed current European Union regulations (Directive 2010/63/EU). Agreement number: B1301310. Neurons used in this study were harvested from the embryos (E15) of Wistar rats. Embryos were collected and immediately placed in ice-cold L15 Leibovitz medium with a 2% penicillin (10,000 U/mL) and streptomycin (10 mg/mL) solution (PS) and 1% bovine serum albumin (BSA).

Primary culture of cortical neurons

Cortices were treated for 20 min at 37 °C with a trypsin-EDTA solution at a final concentration of 0.05% trypsin and 0.02% EDTA. The dissociation was stopped by addition of Dulbecco's modified Eagle's medium (DMEM) with 4.5 g/L of glucose, containing DNAse I grade II (final concentration 0.5 mg/mL) and 10% fetal bovine serum (FBS). Cells were mechanically dissociated by three forced passages through the tip of a 10-mL pipette. Cells were then centrifuged at 515×*g* for 10 min at 4 °C. The supernatant was discarded, and the pellet was resuspended in a defined culture medium consisting of Neurobasal medium with a 2% solution of B27 supplement, 2 mM of L-glutamine, 2% of PS solution, and 10 ng/mL of brain-derived neurotrophic factor (BDNF). Viable cells were counted in a Neubauer cytometer, using the trypan blue exclusion test. The cells were seeded at a density of 25,000 per well in 96-well plates precoated with poly-L-lysine and were cultured at 37 °C in an air (95%)-CO2 (5%) incubator. Half of the medium was changed every other day.

$A\beta_{1-42}$ preparation

$A\beta_{1-42}$ peptide (Bachem) was dissolved in the defined culture medium mentioned above, at an initial concentration of 20 μM. This solution was gently agitated for 3 days at 37 °C in the dark and immediately used after being properly diluted in culture medium to the concentrations used (15 μM, containing 2 μM Aβ oligomers, evaluated by WES™) (for detail, see Callizot et al. 2013 [19]).

$A\beta_{1-42}$ neurotoxicity assay: survival, network, and tau phosphorylation

On day 11 of culture, neurons were treated with at 100 nM fosgo-AM or vehicle (culture medium containing 0.1% DMSO supplemented with 0.05 ng/mL HGF) for 15 min and challenged with $A\beta_{1-42}$ solution (15 μM, containing 2 μM Aβ oligomers) for 24 h. After 24 h, the cell culture supernatant was removed, and the cells were fixed in a solution containing 4% paraformaldehyde in PBS (pH = 7.3) for 20 min at room temperature. The cells were washed twice in PBS, permeabilized and non-specific sites were blocked with a solution of PBS containing 0.1% of saponin and 1% FCS for 15 min at room temperature. The cultures were then incubated with a chicken polyclonal anti-MAP2 antibody and a mouse polyclonal anti-AT100 antibody at dilution of 1:400 in PBS containing 1% FCS, and 0.1% saponin for 2 h at room temperature. Antibodies were detected with Alexa Fluor 488 goat anti-mouse IgG at a dilution of 1:400 and Alexa Fluor 568 goat anti-chicken IgG at a dilution of 1:400 in PBS containing 1% FCS, and 0.1% saponin for 1 h at room temperature. Cell nuclei were counterstained with Hoechst dye (1:1000, Sigma-Aldrich). For each condition, 20 pictures (representing the whole well area) were automatically taken using ImageXpress® (Molecular Devices) at 10x magnification using the same acquisition parameters. Analyses were directly and automatically performed by MetaXpress® (Molecular Devices) to quantify the following read-outs: 1) total number of neurons (MAP2+ neurons), 2) neurite network (total length of MAP2+ in μm), and 3) hyperphosphorylated tau (overlap of MAP2+ and AT100 in μm2).

$A\beta_{1-42}$ neurotoxicity assay: mitochondrial stress

To assess mitochondrial stress via reactive oxygen species (ROS) production, cortical neurons were treated with fosgo-AM (10 nM, 100 nM, or 1 μM) or vehicle (culture medium containing 0.1% DMSO supplemented with 0.05 ng/mL HGF) for 15 min and challenged with $A\beta_{1-42}$ solution (15 μM, containing 2 μM Aβ oligomers) for 4 h. After 4 h, the cell culture supernatant was discarded, and live cells were incubated with MitoSox™ Red (marker of ROS generated by the mitochondria) for 10 min at 37 °C. The MitoSox™ reagent is cell-penetrant and becomes fluorescent once oxidized by superoxide.

Cells were fixed in a cold solution containing 95% ethanol and 5% acetic acid for 5 min at −20 °C. The cells were washed twice with PBS, cell membranes were permeabilized, and non-specific binding sites were blocked with a solution of PBS containing 0.1% saponin and 1% FBS for 15 min at room temperature. Cultures were incubated with a chicken

polyclonal antibody anti microtubule-associated-protein 2 (MAP2) at a dilution of 1:400 in PBS containing 1% FBS and 0.1% of saponin. The antibody was detected with Clear Fluor (CF) 568 goat anti-chicken IgG at a dilution of 1:400 in PBS containing 1% FBS and 0.1% saponin for 1 h at room temperature. Nuclei were counterstained with the fluorescent dye Hoechst (Sigma-Aldrich, 1:1000): marker of cell number. For each condition, 20 pictures (representing the whole well area) were automatically taken using ImageXpress® (Molecular Devices) at 10x magnification using the same acquisition parameters. Analyses were directly and automatically performed by MetaXpress® (Molecular Devices) to quantify the following read-outs: 1) total number of neurons (MAP2+ neurons), 2) neurite network (total length of MAP2+ in μm), and 3) mitochondrial ROS in neurons (overlap MitoSox and MAP2 in μm^2).

To assess mitochondrial stress via cytochrome *c* release, cortical neurons were treated with fosgo-AM (10 nM, 100 nM, or 1 μM) or vehicle (culture medium containing 0.1% DMSO supplemented with 0.05 ng/mL HGF) for 15 min and challenged with Aβ1-42 solution (15 μM, containing 2 μM Aβ oligomers) for 4 h. After 4 h, the cell culture supernatant was discarded, and cells were washed with cold PBS and fixed in a solution of 4% paraformaldehyde in PBS (pH = 7.3) for 20 min at room temperature. The cells were washed twice in PBS, cell membranes were permeabilized, and non-specific binding sites were blocked with a solution of PBS containing 0.1% saponin and 1% FBS for 15 min at room temperature. The cultures were incubated for 2 h at room temperature with a chicken polyclonal antibody anti-microtubule-associated-protein 2 (MAP2) at dilution of 1:400 in PBS containing 1% FBS and 0.1% of saponin and a polyclonal anti-CytC antibody produced in rabbit at dilution of 1:100 in PBS containing 1% FBS and 0.1 % saponin. These antibodies were detected with CF 488 goat anti-mouse IgG at the dilution of 1:800 and with CF 568 goat anti-rabbit IgG at the dilution 1:400 in PBS containing 1% FBS and 0.1% saponin for 1 h at room temperature. Nuclei were counterstained with the fluorescent dye Hoechst (Sigma-Aldrich, 1:1000): marker of cell number. For each condition, 20 pictures (representing the whole well area) were automatically taken using ImageXpress® (Molecular Devices) at 10x magnification using the same acquisition parameters. Analyses were directly and automatically performed by MetaXpress® (Molecular Devices) to quantify the following read-outs: 1) total number of neurons (MAP2+ neurons), 2) neurite network (total length of MAP2+ in μm), and 3) cytochrome *c* release in neuron cytoplasm (overlap CytC and MAP2 in μm^2).

$A\beta_{1-42}$ neurotoxicity assay: protein analysis

To investigate expression levels or phosphorylation status of intracellular proteins, cortical neurons were plated in 24-well plates and treated with fosgo-AM (10 nM, 100 nM, or 1 μM) or vehicle (culture medium containing 0.1% DMSO supplemented with 0.05 ng/mL HGF), challenged with $A\beta_{1-42}$ solution (15 μM, containing 2 μM Aβ oligomers) for 24 h, and Simple Western was conducted to assess proteins of interest. Cells were lysed with a defined buffer lysis consisting of CelLyticMT reagent with 1% protease and phosphatase inhibitor cocktail (60 μl per well). For each condition, the quantity of protein was determined using the micro kit BCA (Pierce). Briefly, lysates were diluted at 1:20 in PBS and mixed, in equal volume, with a micro-BCA working reagent. Solutions were then incubated at 60 °C for 1 h and the quantity of protein was measured at 562 nm with a spectrophotometer Nanovue (GE Healthcare) and compared with the standard of Bovine Serum Albumin curve (BSA, Pierce). All reagents (Ref: SM-W002) (except primary antibodies) and secondary antibodies (Ref: DM-001 or DM-002) were provided by ProteinSimple®. Reagents were prepared and used according to manufacturer's recommendations for use on WES™ (ProteinSimple, USA). The assay was performed according to manufacturer's recommendations. Capillaries, samples, antibodies, and matrices were then loaded inside the instrument. The Simple Western was run with capillaries filled with separation matrix, stacking matrix, and protein samples. Next, capillaries were incubated for 2 h with primary antibodies. The levels of the following proteins were investigated: Glycogen synthase kinase 3 beta (GSK3β), total; GSK3β, phospho-Ser389 (non-active form); GSK3β, phospho-Tyr216 (active form); phospho-tau (pTau [Thr212, Ser214] via AT100); AKT, total; AKT, phospho-Ser473; ERK, total; ERK, phospho-ERK (1/2); Beclin-1, total; ULK1, total. Total GAPDH was analyzed as a housekeeping gene. Each protein was evaluated independently in a separate capillary system. Capillaries were washed and incubated with HRP conjugated secondary antibodies for 1 h. After removal of the unbound secondary antibody, the capillaries were incubated with the luminol-S/peroxide substrate and chemiluminescent signal was collected using the Charge-Coupled Device (CCD) camera of WES™ with six different exposure times (30, 60, 120, 240, 480, and 960 s). Data analysis was performed using the Compass Software (ProteinSimple, USA) on WES™. Four samples (biological replicates) per condition were analyzed. The design did not include technical replicates.

Glutamate neurotoxicity assay: survival, network, and tau phosphorylation

On day 13 of culture, cortical neurons were treated with at 100 nM fosgo-AM or vehicle (culture medium containing 0.1% DMSO supplemented with 0.05 ng/mL HGF) for 20 min and challenged with glutamate (20 μM) for 24 h. After 24 h, the cell culture supernatant was removed, and the cells were fixed in a solution containing 4% paraformaldehyde in PBS (pH = 7.3) for 20 min at room temperature. The cells were washed twice in PBS, permeabilized, and non-specific sites were blocked with a solution of PBS containing 0.1% of saponin and 1% FCS for 15 min at room temperature. The cultures were then incubated with a chicken polyclonal anti-MAP2 antibody and a mouse polyclonal anti-AT100 antibody at dilution of 1:400 in PBS containing 1% FCS, and 0.1% saponin for 2 h at room temperature. Antibodies were detected with Alexa Fluor 488 goat anti-mouse IgG at the dilution 1:400 and Alexa Fluor 568 goat anti-rabbit IgG at the dilution 1:400 in PBS containing 1% FCS, and 0.1% saponin for 1 h at room temperature. Cell nuclei were counterstained with Hoechst dye (1:1000, Sigma-Aldrich). For each condition, 20 pictures (representing the whole well area) were automatically taken using ImageXpress® (Molecular Devices) at 10x magnification using the same acquisition parameters. Analyses were directly and automatically performed by MetaXpress® (Molecular Devices) to quantify the following read-outs: 1) total number of neurons (MAP2+ neurons), 2) neurite network (total length of MAP2+ in μm), and 3) hyperphosphorylated tau (overlap of MAP2+ and AT100 in μm2). In a separate culture, treatment groups included GSK-960693 (pan-AKT inhibitor) or PD98059 (selective inhibitor of the MEK/ERK pathway) to determine the neuroprotective effect of fosgo-AM on neuronal total number of neurons (MAP2+ neurons) or neurite network (total length of MAP2+ in μm) following glutamate injury and under AKT or MEK/ERK inhibition.

Statistical analysis

All values are expressed as mean ± SEM (standard error of the mean). Normality was verified (Shapiro-Wilke), and Grubb's test was utilized to identify any outliers. For immunocytochemistry experiments, N = 3 biological replicates (independent preparations of cortical neurons), n = 4–6 technical replicates. For Western blot experiments, N = 3–4 biological replicates. Statistical differences were analyzed by one-way ANOVA followed by Fisher's least significant differences (LSD) or Dunnett's multiple comparisons test (Prism GraphPad). *p < 0.05, **p < 0.01, ***p < 0.001, ****p < 0.0001 vs. relevant controls as indicated.

ICV-$A\beta_{25-35}$ rat model of cognitive impairment

Animals

Adult male Wistar rats (weighing approximately 210 g at study start) were used to assess Aβ-induced cognitive impairment. Rats were group housed at 3 per cage and maintained in a temperature-controlled room with reverse light-dark cycle (12:12). Food and water were available *ad libitum*. Animals were assigned to groups pseudo-randomly prior to surgery with 12 rats per group (total of 96 rats). The groups were: Sham +

Vehicle, ICV-Aβ + Vehicle, and ICV-Aβ + Fosgonimeton at 0.125 mg/kg, 0.25 mg/kg, 0.5 mg/kg, 1 mg/kg, or 2 mg/kg. All animal manipulations were conducted in accordance with the European Directive 2010/63/UE published in the French decree 2013-118 of February 1, 2013, and approved by an independent government-accredited ethics committee (CEEA 35, NEUROFIT, France).

Drug preparation and treatment

Aβ peptide fragment 25–35 was dissolved in water at 3 μg/μL and stored at −80 ° Celsius (C). Then, for the 5 days prior to surgery, the peptide in solution was incubated at 37 °C to allow fibrillation. Thirty minutes prior to surgery, animals received a subcutaneous injection of 0.02 mg/kg of buprenorphine. Rats were anesthetized with 2.5–3% isoflurane and secured in a stereotaxic frame. Then, 5 μL of fibrillated Aβ was injected into the right ventricle (AP -0.8, ML -1.5, DV -4.2). For pain management, rats received additional buprenorphine doses in the evening and morning following the surgery. Fosgonimeton was dissolved in saline and administered at a dosing volume of 1 mL/kg at final concentrations of 0.125 mg/kg, 0.25 mg/kg, 0.5 mg/kg, 1 mg/kg, and 2 mg/kg. Fosgonimeton or vehicle was delivered daily via the subcutaneous route from the day of surgery (study day 0) until study day 14 (following passive avoidance acquisition).

Passive avoidance test

The passive avoidance apparatus is an elevated runway separated from a dark compartment by a small door. The grid floor of the dark compartment is connected to an electrical shock generator. The apparatus is a 27 × 25 × 27 (L × W × H) cm chamber with grey opaque walls. The floor of the box is constructed of fifteen stainless steel rods spaced approximately 1.2 cm apart. The top of the chamber is covered by an opening door made with the same material as the wall. The front wall of the chamber is connected to a runway of 50 cm length and 8 cm width on a plane with the grid floor. Passage from the elevated runway into the box is through an opening of 8 cm wide and 9 cm high. A movable door is provided to obstruct the box entrance. The apparatus is elevated at 75 cm from the ground.

During the acquisition session (study day 14), the far end of the runway was brightly illuminated so as to be aversive to the rat. Rats were placed onto the far end of the runway facing away from the dark compartment. Once the rat fully entered the dark compartment, the door closed, and a mild foot shock (0.5 mA) was delivered through the grid floor for 5 s. The rat then remained in the dark compartment for 30 s following the foot shock. The acquisition session did not end until the rat stayed on the elevated runway for 120 s or until 5 trials elapsed. The retention test took place 24 h following acquisition (study day 15). During the retention test, rats were evaluated for the time it took to enter the dark compartment (step-through latency). No shock was delivered during the retention test. The retention trial ended after the rat entered the dark compartment or after 300 s.

Statistical analysis

Values are expressed as mean ± SEM (standard error of the mean). Statistical analysis was performed by one-way ANOVA followed by Dunnett's multiple comparisons test. *p < 0.05, **p < 0.01, ***p < 0.001, ****p < 0.0001 vs. ICV-Aβ + Vehicle.

Results

Fosgo-AM promotes neuronal survival, preserves neurite networks, and reduces tau hyperphosphorylation following A$\beta_{1\text{-}42}$ injury

To evaluate neuroprotective effects of fosgonimeton against Aβ-mediated toxicity, primary cortical neurons were treated with the active metabolite of fosgonimeton, fosgo-AM, for 15 min and incubated with A$\beta_{1\text{-}42}$ solution for 24 h. Co-immunostaining of the neuronal marker MAP2 and hyperphosphorylated tau (pTau [Thr212, Ser214]) marker AT-100 was performed to determine neuronal survival (i.e., number of neurons), neurite network (i.e., total length of neurites), and levels of pTau (Fig. 1a). As expected, exposure to A$\beta_{1\text{-}42}$ resulted in a significant decrease in the number of neurons (64 ± 1.0% of normal control; Fig. 1b) and total length of neurites (63 ± 1.0% of normal control; Fig. 1c). Such effects were significantly attenuated in the presence of fosgo-AM; that is, treatment with fosgo-AM led to a significant increase in neuronal survival (79 ± 2% of normal control; Fig. 1b) and neurite network (83 ± 2% of normal control; Fig. 1c), compared to the A$\beta_{1\text{-}42}$ control. Moreover, cultures treated with fosgo-AM had significant reductions in the levels of pTau (150 ± 2% of normal control; Fig. 1d), compared to the A$\beta_{1\text{-}42}$ control (203 ± 6% of normal control). Taken together, these observations highlight the potential of fosgonimeton to mitigate neurotoxic Aβ pathology.

Fosgo-AM attenuates Aβ-induced mitochondrial oxidative stress and apoptotic signaling

Mitochondrial dysfunction is a major pathogenic event underlying Aβ toxicity [2,17,18,41,42]. To assess whether the neuroprotective effects of fosgonimeton could attenuate Aβ-mediated mitochondrial dysfunction and characterize a potential mechanism by which fosgonimeton mitigates neurotoxicity, primary cortical neurons were treated with fosgo-AM for 15 min and challenged with A$\beta_{1\text{-}42}$ for 4 h (a time point at which Aβ-induced neuronal death has yet to occur [19]) and immunoassayed with anti-MAP2 and either MitoSox (an indicator of ROS generated by the mitochondria) (Fig. 2a and b), or anti-CytC (marker of cytochrome *c*) (Fig. 2c and d). Cytochrome *c* is a highly conserved protein found on the inner membrane of the mitochondrion where it regulates cellular respiration. Under mitochondrial oxidative stress, cytochrome *c* is released into the cytoplasm where it interacts with apoptotic proteins resulting in caspase activation and eventual cell death [43]. Consistent with previous observations, A$\beta_{1\text{-}42}$ treatment did not induce any neuronal loss (Fig. S1a) or neurite degeneration (Fig. S1b) at this early stage. However, treatment with A$\beta_{1\text{-}42}$ resulted in a significant increase in mitochondrial ROS (155 ± 2% of normal control; Fig. 2b) and release of cytochrome *c* (127 ± 1% of normal control; Fig. 2d) highlighting an early mechanism of dysfunction [43]. In the presence of 100 nM fosgo-AM, however, mitochondrial ROS and release of cytochrome *c* triggered by A$\beta_{1\text{-}42}$ remained near control levels: 110 ± 2% (Fig. 2b) and 100 ± 2% of normal control (Fig. 2d), respectively. Such effects are expected to counteract Aβ-mediated toxicity and promote neuronal survival.

Fosgo-AM increases AKT and ERK phosphorylation, and reduces GSK3β activity and tau phosphorylation following A$\beta_{1\text{-}42}$ injury

The serine/threonine kinase AKT is a key mediator of pro-survival, anti-apoptotic, and neurotrophic signaling [44–46]. Dysfunction in AKT signaling has been linked to Aβ toxicity as it blunts pro-survival signaling and renders neurons vulnerable to neurological stressors [22]. To assess if positive modulation of HGF by fosgo-AM engages AKT signaling to protect neurons from Aβ toxicity, cortical neurons were treated with fosgo-AM and A$\beta_{1\text{-}42}$, and Simple Western was conducted to assess phosphorylated AKT (pAKT [Ser473]) and total AKT (Fig. 3a). Quantification of Simple Western revealed a significant decrease in the ratio of pAKT normalized to AKT$_{total}$ in neuronal cultures treated with A$\beta_{1\text{-}42}$ (60 ± 6% of normal control; Fig. 3b). Treatment with fosgo-AM significantly increased the ratio of pAKT/AKT$_{total}$, restoring it to levels similar to those observed under normal control conditions (maximal effect 100 nM fosgo-AM, 91 ± 6% of normal control; Fig. 3b).

Due to the critical role of ERK signaling in neuroprotection [36,47], synaptic plasticity [48], and memory formation [49], we also investigated the effect of fosgo-AM on ERK activation. Protein levels of phosphorylated ERK (pERK [Thr202, Tyr204]) and total ERK were evaluated following A$\beta_{1\text{-}42}$ challenge in the presence or absence of fosgo-AM (Fig. 3c). Quantification indicated that neuronal cultures treated with A$\beta_{1\text{-}42}$ exhibited a significant increase in pERK/ERK$_{total}$ ratio (136 ± 9%

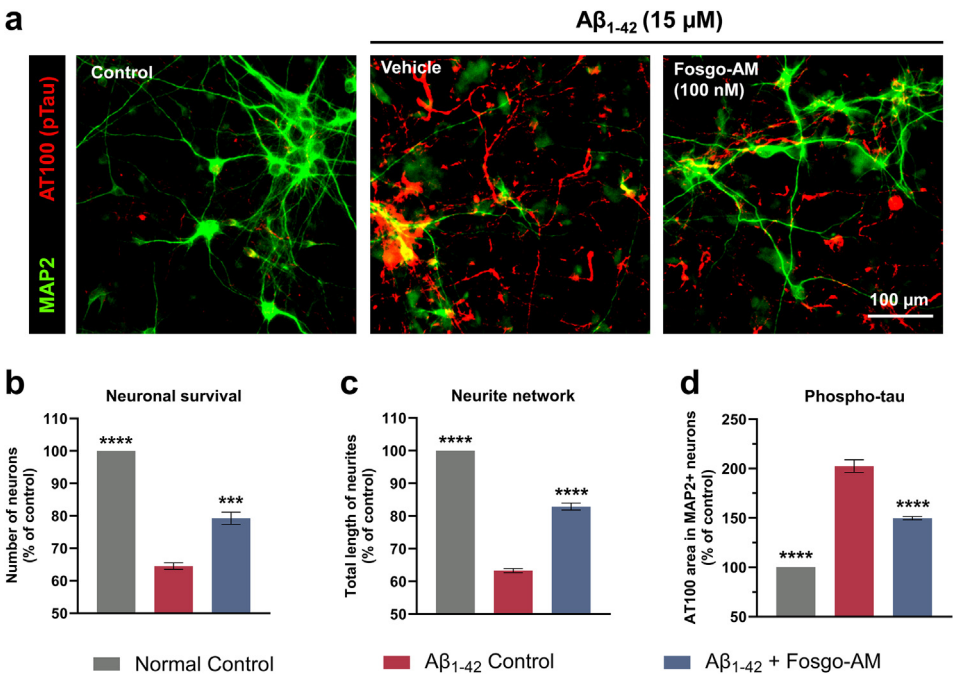

Fig. 1. Fosgo-AM promotes neuronal survival, preserves neurite networks, and reduces tau hyperphosphorylation following $A\beta_{1\text{-}42}$ injury. Primary rat cortical neurons were treated with the active metabolite of fosgonimeton, fosgo-AM (100 nM), and $A\beta_{1\text{-}42}$ (15 μM; 2 μM oligomers) for 24 h and labeled with microtubule-associated protein-2 (MAP2; neuronal marker) and AT100 (marker for pTau-Thr212/Ser214). Scale bar = 100 μm. (a) Representative images highlighting the effect of $A\beta_{1\text{-}42}$ oligomers on cortical neurons in the presence and absence of fosgo-AM. (b–d) Quantification of neuronal survival (i.e., number of MAP2+ neurons), neurite network (i.e., total length of MAP2+ neurites in μm), and pTau (i.e., overlap of AT100 and MAP2 area in μm^2), expressed as percentage of normal control (100%). Data presented as mean ± SEM; N = 3 biological replicates (independent preparations of cortical neurons), n = 4–6 technical replicates. Statistical differences were determined by one-way ANOVA followed by Fisher's LSD test. ***p < 0.001, ****p < 0.0001 versus $A\beta_{1\text{-}42}$ control.

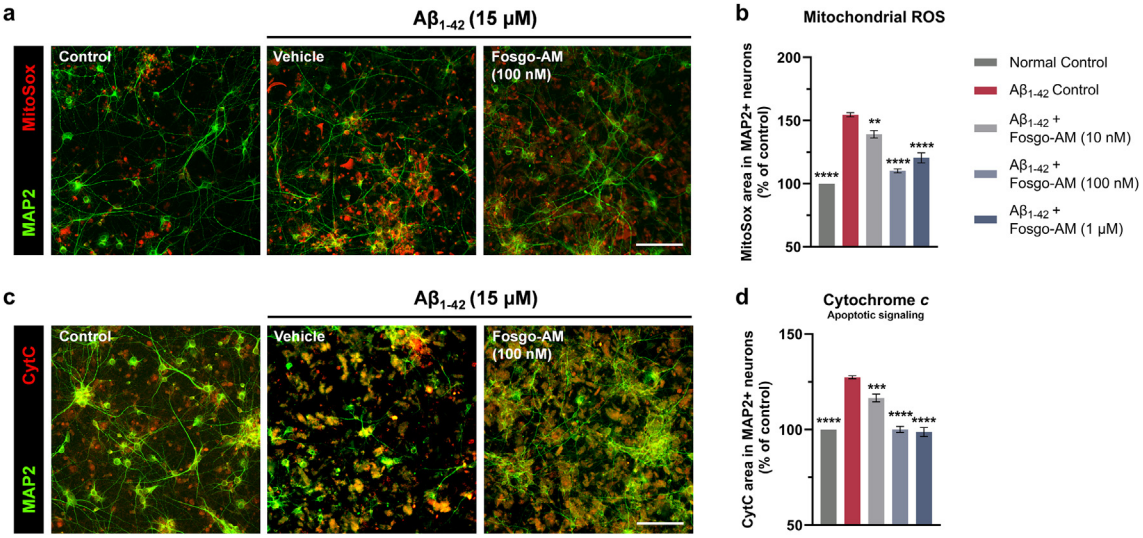

Fig. 2. Fosgo-AM attenuates Aβ-induced mitochondrial oxidative stress and cytochrome *c* release. (a) Primary rat cortical neurons were treated with the active metabolite of fosgonimeton, fosgo-AM, and $A\beta_{1\text{-}42}$ (15 μM; 2 μM oligomers) for 4 h and labeled with microtubule-associated protein-2 (MAP2; neuronal marker) and MitoSox (marker of mitochondrial ROS). Scale bar = 100 μm. (b) Quantification of mitochondrial ROS (i.e., overlap of MitoSox and MAP2 area), expressed as percentage of normal control (100%). (c) Primary rat cortical neurons were treated with the fosgo-AM and $A\beta_{1\text{-}42}$ (15 μM; 2 μM oligomers) for 4 h and labeled with MAP2 and anti-CytC (marker of cytochrome *c*). Scale bar = 100 μm. (d) Quantification of cytochrome *c* release (i.e., overlap of CytC and MAP2 area), expressed as percentage of normal control (100%). Data presented as mean ± SEM; N = 3 biological replicates (independent preparations of cortical neurons), n = 4–6 technical replicates. Statistical differences were determined by one-way ANOVA followed by Fisher's LSD test. **p < 0.01, ***p < 0.001, ****p < 0.0001 versus $A\beta_{1\text{-}42}$ control.

of normal control; Fig. 3d). Consistent with our previous observations [40], treatment with fosgo-AM induced a robust increase in ERK phosphorylation (maximal effect at 1 μM fosgo-AM, 229 ± 15% of normal control; Fig. 3d).

A critical component of Aβ pathology is increased activity of GSK3β, one of the main kinases involved in the hyperphosphorylation of tau [51, 52]. To assess GSK3β activity, we measured levels of GSK3β phosphorylated on Tyrosine 216 (corresponding to the active form of GSK3β) and Serine 389 (corresponding to the inactive form of GSK3β) and evaluated the ratio of $pGSK3\beta^{Y216}$ to $pGSK3\beta^{S389}$ (active to inactive) (Fig. 3e). As expected, $pGSK3\beta^{Y216}/pGSK3\beta^{S389}$ was significantly increased in cortical neurons after a 24-h $A\beta_{1\text{-}42}$ application (217 ± 17% of normal control; Fig. 3f). Treatment with 100 nM fosgo-AM significantly blunted this effect (117 ± 3% of normal control; Fig. 3f). $A\beta_{1\text{-}42}$ exposure also led to a concomitant increase in the level of hyperphosphorylated tau (179 ± 10% of control conditions; Fig. 3g and h), an effect that was also significantly reduced in the presence of fosgo-AM (maximal effect at 10 nM fosgo-AM, 85 ± 10% of normal control; Fig. 3g and h). These observations provide mechanistic insight on the ability of fosgonimeton to counteract Aβ-mediated cellular dysfunction via promotion of pro-survival signaling and reduction of pathological tau in cortical neuron culture.

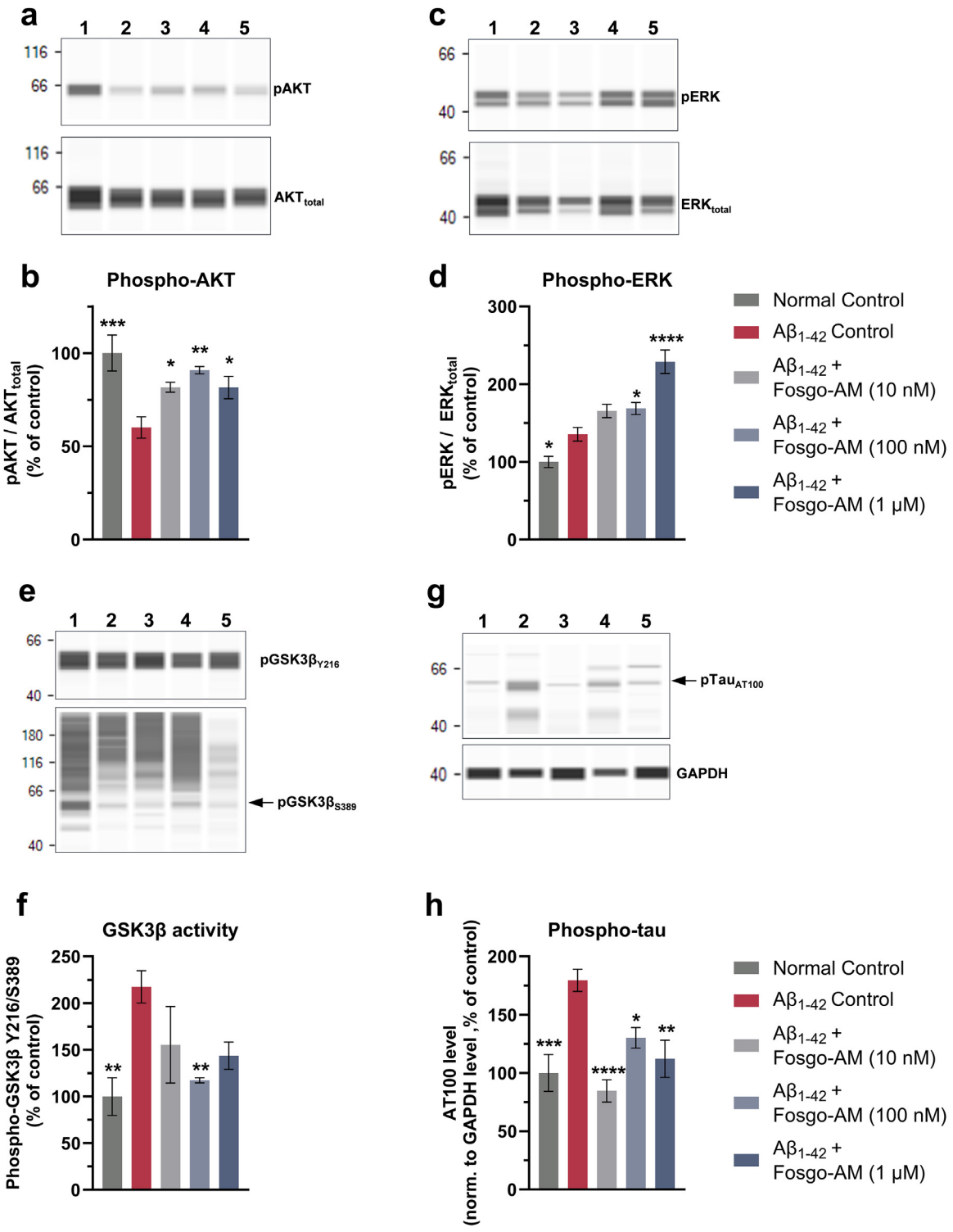

Fig. 3. Fosgo-AM increases AKT and ERK phosphorylation and reduces GSK3β activity and tau phosphorylation following $A\beta_{1-42}$ injury. Primary rat cortical neurons were treated with the active metabolite of fosgonimeton, fosgo-AM, and $A\beta_{1-42}$ (15 μM; 2 μM oligomers) for 24 h and protein lysates were analyzed for total AKT, phospho-AKT ($pAKT^{Ser473}$), total ERK, phospho-ERK ($pERK^{Thr202/Tyr204}$), and phospho-GSK3β ($pGSK3\beta^{Tyr216}$ or $pGSK3\beta^{Ser389}$), or phospho-Tau ($pTau^{Thr212/Ser214}$) via Simple Western. (a, b) Representative images of Simple Westerns and corresponding quantification showing AKT phosphorylation as pAKT/AKT. (c, d) Representative images of Simple Westerns and corresponding quantification showing ERK phosphorylation as pERK/ERK. (e, f) Representative images of Simple Westerns and corresponding quantification showing GSK3β activity as $pGSK3\beta^{Tyr216}$(active)/$pGSK3\beta^{Ser389}$(inactive). (g, h) Representative images of Simple Westerns and corresponding quantification showing levels of pTau, normalized to GAPDH level. Borders for representative images highlight that each protein was evaluated independently in a separate capillary system. Lanes: 1, normal control; 2, $A\beta_{1-42}$ control; 3, $A\beta_{1-42}$ + fosgo-AM (10 nM); 4, $A\beta_{1-42}$ + fosgo-AM (100 nM), $A\beta_{1-42}$ + fosgo-AM (1 μM). Data presented as mean ± SEM; N = 3–4 biological replicates (independent preparations of cortical neurons). Statistical differences were determined by one-way ANOVA followed by Fisher's LSD test. *$p < 0.05$, **$p < 0.01$, ***$p < 0.001$, ****$p < 0.0001$ versus $A\beta_{1-42}$ control.

Fosgo-AM increases autophagy markers ULK1 and Beclin-1 following $A\beta_{1-42}$ injury

Impairments in autophagy, the main mechanism by which neurons degrade and clear insoluble protein aggregates, are well documented in AD pathogenesis [53–55]. Thus, we sought to investigate the effect of fosgo-AM on autophagy markers following $A\beta_{1-42}$ injury. We focused on two proteins that are central to the initiation of autophagy and have been linked to Aβ pathology: Unc-like Kinase 1 (ULK1) and Beclin-1. Beclin-1 regulates both autophagosome synthesis and maturation [56], and is activated by ULK1-mediated phosphorylation [57,58]. Simple Western was utilized to evaluate the effect of fosgo-AM on ULK1 and Beclin-1 expression following $A\beta_{1-42}$ challenge. The protein level of ULK1 was significantly decreased in cortical neuron culture 24 h after injury with $A\beta_{1-42}$ (36 ± 6% of normal controls; Fig. 4a and b), suggesting the $A\beta_{1-42}$ interfered with mechanisms governing initiation of autophagy. This effect was significantly mitigated by treatment with 100 nM fosgo-AM (83 ± 14% of normal control conditions; Fig. 4a and b). Application of $A\beta_{1-42}$ also significantly decreased the level of Beclin-1 (62 ± 9% of normal control; Fig. 4c and d). Treatment with 100 nM fosgo-AM significantly increased Beclin-1 levels, even beyond the normal control level (137 ± 6 % of normal control; Fig. 4c and d). Together, the finding that fosgo-AM was able to prevent Aβ-induced reductions in both ULK1 and Beclin-1 may suggest that fosgo-AM promotes autophagic function, a process that has important implications for the clearance of toxic protein accumulations.

Fosgo-AM protects cortical neurons from excitotoxicity via AKT and ERK signaling

Among the pathological mechanisms promoted by Aβ oligomers, a key driver of neurodegeneration is the excitotoxic overstimulation of excitatory glutamatergic neurotransmission [59]. To evaluate the neuroprotective effects of fosgo-AM on glutamate-induced excitotoxicity, we conducted immunoassays on primary cortical neurons treated with vehicle control, vehicle + glutamate, or fosgo-AM + glutamate using anti-MAP2 and AT100 antibodies (Fig. 5a). Cultures treated with fosgo-AM + glutamate exhibited a significant increase in neuronal survival (80 ± 1% of normal control; Fig. 5b) and neurite network (78 ± 1% of normal control; Fig. 5c) when compared to cultures treated with glutamate only (65 ± 1% of normal control for neuronal survival and 63 ± 3% for neurite network). Furthermore, treatment with fosgo-AM significantly reduced levels of pTau (144 ± 5% of normal control; Fig. 5d) when compared to glutamate treatment alone (200 ± 3% of normal control; Fig. 5d). Overall, these results suggest that fosgo-AM may alleviate excitotoxicity-mediated neuronal damage.

Next, we sought to determine whether the neuroprotective actions of fosgo-AM were mediated by AKT and MEK/ERK signaling. Indeed, the neuroprotective effects of fosgo-AM on neuronal survival (77 ± 1% of normal control; Fig. 6a) were abolished in the presence of GSK-690963 [AKT inhibitor] (67 ± 1% of normal control; Fig. 6a) or PD98059 [MEK/ERK inhibitor] (64 ± 3% of normal control; Fig. 6a). Similar effects were observed on neurite network (Fig. 6b). Collectively, these observations highlight the neuroprotective actions of fosgo-AM against glutamate toxicity, and further strengthen the notion that activation of AKT and ERK signaling are central to the neuroprotective effects of fosgonimeton.

Fosgonimeton rescues cognitive performance in the intracerebroventricular $A\beta_{25-35}$ rat model of AD

Brain accumulation of Aβ peptides in animal models leads to impaired cognitive function [60,61]. As such, the introduction of neurotoxic Aβ peptides into the brains of model species is suitable to determine preclinical efficacy of test compounds under investigation for AD. To evaluate the effects of fosgonimeton on cognitive impairment in vivo, we administered the neurotoxic peptide $A\beta_{25-35}$ or vehicle intracerebroventricularly (ICV) to adult male Wistar rats. The $A\beta_{25-35}$ fragment is recognized as a surrogate for the full-length $A\beta_{1-42}$ peptide, in terms of neurotoxic effects [62]. Fosgonimeton (0.125, 0.25, 0.5, 1, or 2 mg/kg) or vehicle were administered subcutaneously (sc) from day of surgery (study day 0) to study day 14. On study day 14, rats underwent the passive avoidance acquisition paradigm, where entering a darkened compartment is associated with receiving a mild foot shock. A final dose of fosgonimeton or vehicle was administered 1-h after the acquisition trial. This timing was chosen such that the test compound would be on-board during memory consolidation processes, but without introducing the potential confound of injection-related stress on behavior

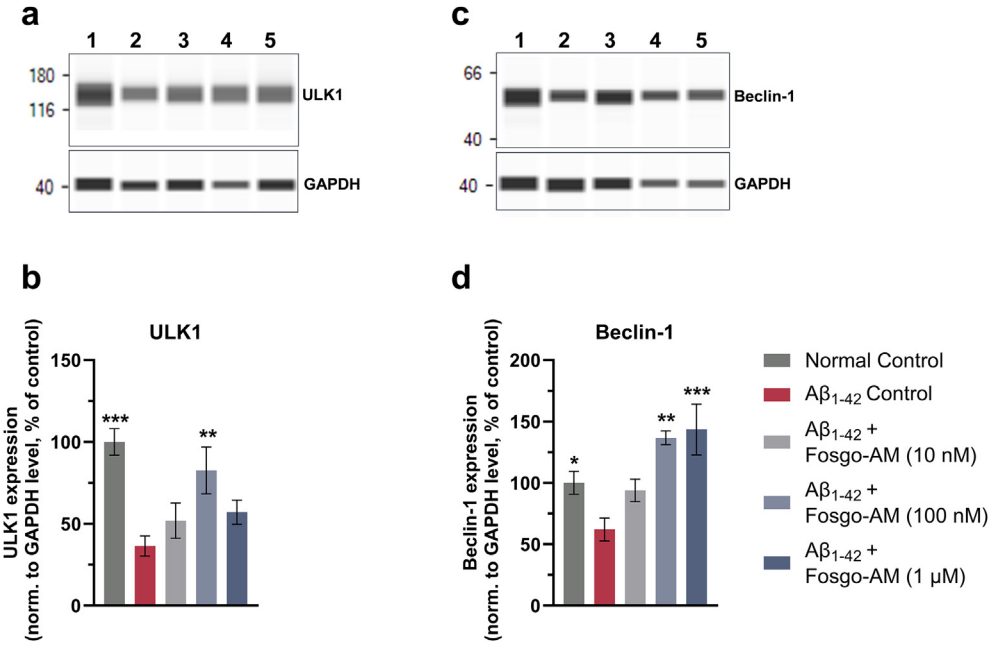

Fig. 4. Fosgo-AM increases levels of ULK1 and Beclin-1 following $A\beta_{1-42}$ injury. Primary rat cortical neurons were treated with the active metabolite of fosgonimeton, fosgo-AM, and $A\beta_{1-42}$ (15 μM; 2 μM oligomers) for 24 h and protein lysates were analyzed for ULK1 and Beclin-1 via Simple Western. (a, b) Representative image of Simple Westerns and corresponding quantification showing levels of ULK1, normalized to GAPDH levels. (c, d) Representative images of Simple Westerns and corresponding quantification showing levels of Beclin-1, normalized to GAPDH levels. Borders for representative images highlight that each protein was evaluated independently in a separate capillary system. Lanes: 1, normal control; 2, $A\beta_{1-42}$ control; 3, $A\beta_{1-42}$ + fosgo-AM (10 nM); 4, $A\beta_{1-42}$ + fosgo-AM (100 nM); 5, $A\beta_{1-42}$ + fosgo-AM (1 μM). Data presented as mean ± SEM; N = 3–4 biological replicates (independent preparations of cortical neurons). Statistical differences were determined by one-way ANOVA followed by Fisher's LSD test. *$p < 0.05$, **$p < 0.01$, ***$p < 0.001$ versus $A\beta_{1-42}$ control.

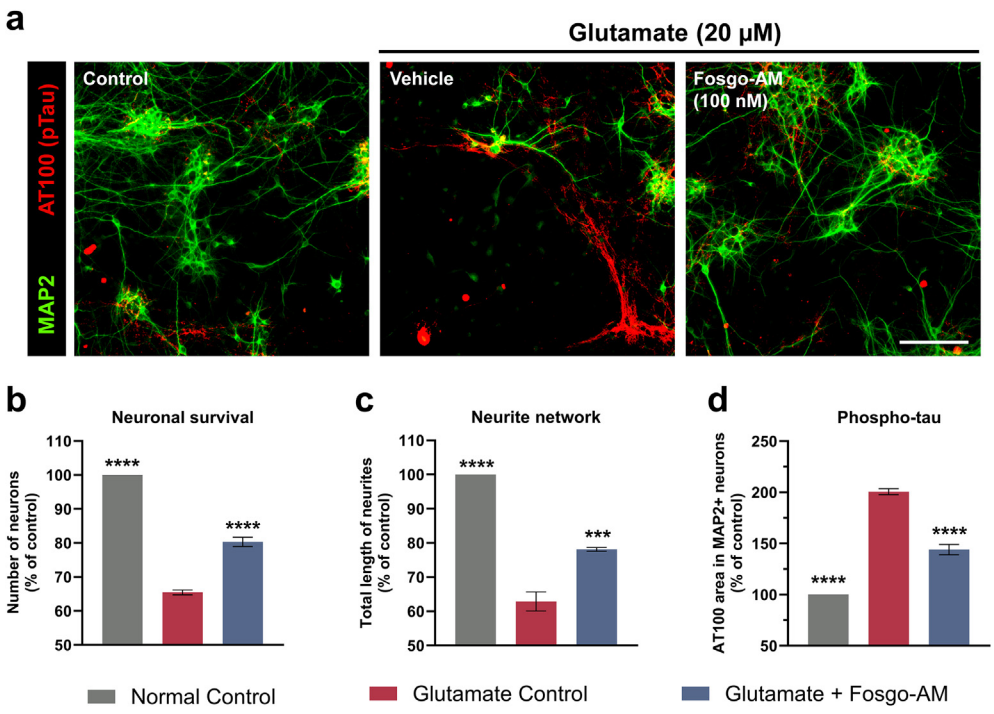

Fig. 5. Fosgo-AM promotes neuronal survival, preserves neurite networks, and reduces tau hyperphosphorylation following glutamate injury. Primary rat cortical neurons were treated with the active metabolite of fosgonimeton, fosgo-AM (100 nM), and glutamate (20 μM) for 24 h and labeled with microtubule-associated protein-2 (MAP2; neuronal marker) and AT100 (marker for pTau). Scale bar = 100 μm. (a) Representative images highlighting the effect of glutamate on cortical neurons in the presence and absence of fosgo-AM. (b–d) Quantification of neuronal survival (i.e., number of MAP2+ neurons), neurite network (i.e., total length of MAP2+ neurites in μm), and pTau (i.e., overlapping area of AT100 and MAP2 in μm^2), expressed as percentage of normal control (100%). Data presented as mean ± SEM; N = 3 biological replicates (independent preparations of cortical neurons), n = 4–6 technical replicates. Statistical differences were determined by one-way ANOVA followed by Fisher's LSD test. ***p < 0.001, ****p < 0.0001 versus glutamate control.

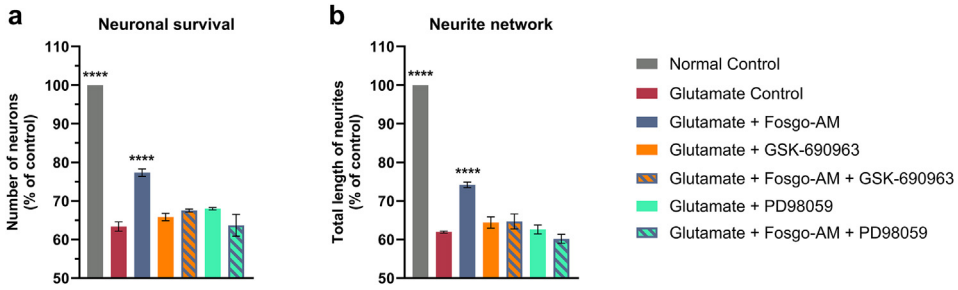

Fig. 6. Neuroprotective actions of fosgo-AM versus glutamate excitotoxicity are mediated by AKT and ERK signaling. Primary rat cortical neurons were treated with AKT inhibitor (GSK-690963) or MEK/ERK inhibitor (PD98059), followed by fosgo-AM (100 nM), and glutamate (20 μM) for 24 h. Cells were labeled with microtubule-associated protein-2 (MAP2; neuronal marker) to assess neuronal survival (i.e., number of MAP2+ neurons) and neurite network (i.e., total length of MAP2+ neurites in μm). (a–b) Effect of fosgo-AM on (a) neuronal survival and (b) neurite networks following glutamate injury, in the presence of the AKT inhibitor or the MEK/ERK inhibitor. Data presented as mean ± SEM; N = 3 biological replicates (independent preparations of cortical neurons), n = 4–6 technical replicates. Statistical differences were determined by one-way ANOVA followed by Dunnett's multiple comparisons test. ****p < 0.0001 versus glutamate control.

during the trial itself. On study day 15, rats were again placed into the passive avoidance apparatus and assessed for step-through latency in a memory retention trial. ICV-Aβ-exposed rats exhibited significantly reduced step-through latency times in the passive avoidance test compared to sham surgery control rats, indicating poor retention of the previously learned association, and therefore cognitive impairment. Treatment with fosgonimeton significantly restored cognitive function at all doses tested (Fig. 7a). The maximum average degree of recovery with fosgonimeton treatment was 88% recovery in 0.125 mg/kg treated group (Fig. 7b). Overall, treatment with fosgonimeton led to significant cognitive rescue in the ICV- $A\beta_{25-35}$ rat model of AD, indicating that the cellular effects of fosgonimeton translate to functional benefits in vivo.

Discussion

We have previously reported on the ability of fosgonimeton, a small-molecule positive modulator of the neurotrophic HGF signaling system, to promote neurotrophic and neuroprotective effects in primary neuron culture and rescue cognitive impairment induced by cholinergic deficits and neuroinflammation in rodents [40]. Herein, we show that positive modulation of the HGF system by fosgonimeton also attenuates pathological alterations downstream of Aβ in vitro and in vivo. Our data suggest that such effects are driven by the ability of fosgonimeton to stimulate pro-survival signaling cascades that counteract oxidative stress, mitochondrial dysfunction, apoptotic signaling, and pathological protein accumulation. These multimodal actions highlight the potential of fosgonimeton as a disease-modifying therapeutic for the treatment of AD.

$A\beta_{1-42}$-induced cytotoxicity has been associated with disruption of mitochondrial membrane potential and production of ROS, leading to the induction of apoptotic mechanisms [2,17,18,41,42]. Upregulation of ROS and apoptotic signaling trigger several neurodegenerative events including synapse loss, neurite degeneration, pathological protein accumulation, and neuroinflammation. In our mitochondrial stress assays, we observed that fosgo-AM significantly blunts the initial Aβ-mediated

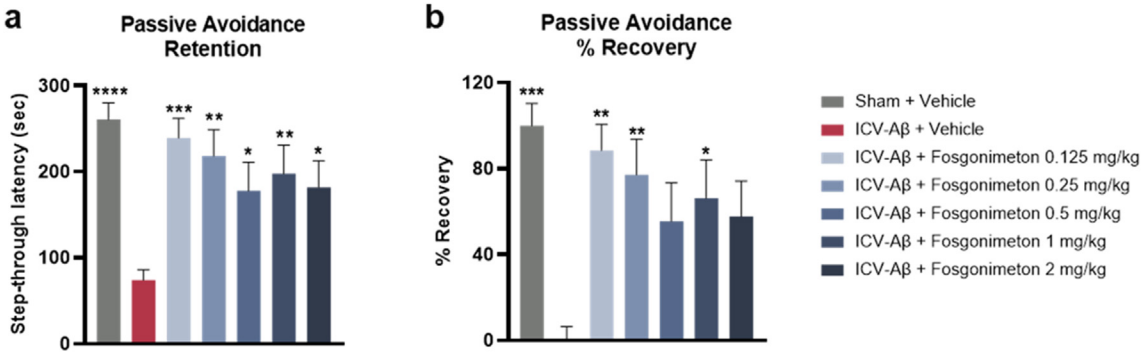

Fig. 7. Fosgonimeton improves cognitive performance in passive avoidance retention in ICV-A$\beta_{25\text{-}35}$-exposed rats. Cognitive performance was assessed in rats administered with ICV-A$\beta_{25\text{-}35}$ or sham and treated with fosgonimeton or vehicle for 14 days. (a) Step-through latency in passive avoidance retention trial. Fosgonimeton at all tested doses resulted in significant rescue of cognitive impairment, as indicated by longer step-through latencies. (b) Data presented as percent recovery, normalized to Sham + Vehicle (100%) and ICV-Aβ + Vehicle (0%) groups. Data presented as mean ± SEM; n = 12 rats per group. Statistical differences were determined by one-way ANOVA followed by Dunnett's multiple comparisons test for step-through latency, and by Kruskal-Wallis followed by Dunn's multiple comparisons for percent recovery. *p < 0.05, **p < 0.01, ***p < 0.001, ****p < 0.0001 versus ICV-Aβ + Vehicle.

increased levels of ROS and cytochrome *c* release. Mechanistic insight regarding such an effect may be gleaned from our observations on AKT and ERK signaling [36]. We have previously demonstrated that positive modulation of the HGF/MET system by fosgo-AM enhances phosphorylation of AKT and ERK and protects cortical neurons from cytotoxicity induced by several neurological stressors implicated in neurodegeneration [40]. We posited that activation of AKT and ERK signaling may, in part, underlie the neuroprotective actions of fosgo-AM. Indeed, neuronal cultures treated with fosgo-AM exhibited a significant increase in AKT and ERK phosphorylation following Aβ injury, thereby suggesting engagement of pro-survival signaling downstream of HGF/MET. The neuroprotective and anti-apoptotic effects of HGF via AKT and ERK signaling have been reported [36] and provide a plausible mechanism for the ability of fosgonimeton to counteract Aβ-mediated mitochondrial ROS and cytochrome *c* release. For instance, activation of AKT can upregulate the expression of anti-apoptotic Bcl-2 proteins, inhibit pro-apoptotic proteins such as Bid and BAD, and/or prevent release of cytochrome *c* and caspase activation [45,63]. Not surprisingly, reduction of AKT signaling is thought to play a role in the early cellular dysfunction associated with Aβ pathology, as it diminishes the aforementioned pro-survival responses [22]. With regards to ERK signaling, Aβ has been shown to interact with cell surface receptors, such as NMDA, mGluR5, and α7 nicotinic receptors leading to ERK phosphorylation [50]. The consequences of ERK activation in response to Aβ may depend on several factors including the mechanism by which ERK is activated, the cell type, the duration of ERK activation, and/or subcellular localization. It has been suggested that increased ERK activation in response to Aβ may represent a compensatory mechanism to counteract AD-related pathology [50]. In agreement with previous reports, we observed a significant increase in pERK after Aβ treatment, and fosgo-AM led to a further increase in pERK. Given that HGF-mediated activation of ERK signaling has been shown to play a role in neuroprotection and synaptic plasticity [36], we posit that activation of ERK by fosgonimeton promotes neuroprotective activity that counteracts Aβ-mediated toxicity. Taken together, our data suggest that fosgonimeton counteracts pathological oxidative changes that could otherwise lead to neurodegeneration, and that such effects may be due to activation of AKT and ERK signaling.

Activation of AKT and ERK has also been implicated in the neuroprotective mechanisms against other Aβ-related pathologies such as glutamate excitotoxicity [64–66]. Aβ pathology has been shown to modulate the expression and/or function of several glutamate receptors (e.g., NMDA) and transporters (e.g., excitatory amino acid transporter-2) leading to an abnormal increase of glutamate in the synaptic cleft, neurotransmission disturbances, and activation of extra-synaptic glutamate receptors [16,59,67]. Activation of extra-synaptic glutamate receptors can trigger pathological elevation of intracellular Ca^{2+} concentrations and activation of Ca^{2+}-dependent enzymatic pathways leading to mitochondrial dysfunction, oxidative stress, and tau phosphorylation [67,68]. To reinforce the involvement of the AKT and ERK pathways in the mechanism of action of fosgonimeton, we inhibited AKT and MEK/ERK and evaluated the neuroprotective effect of fosgo-AM in primary culture directly challenged with glutamate to model this pathogenic event. In corroboration with our previous observation that fosgo-AM protects cortical neurons from glutamate toxicity [40], treatment with fosgo-AM led to increased cortical neuron survival and neurite network integrity following glutamate injury. Fosgo-AM also attenuated glutamate-induced tau hyperphosphorylation. Importantly, the neuroprotective effects of fosgo-AM were abolished in the presence of AKT or MEK/ERK inhibitors, confirming the direct involvement of these signaling pathways in the downstream mechanism of action of fosgonimeton.

Aβ oligomers are known to dysregulate various kinases and phosphatases that can in turn upregulate the phosphorylation of tau [14,23]. Indeed, we observed that application of A$\beta_{1\text{-}42}$ increased the activity of GSK3β and upregulated tau phosphorylation. Both of those effects were significantly attenuated in the presence of fosgo-AM. While the exact mechanism by which fosgo-AM modulates GSK3β activity is yet to be elucidated, these observations are of critical importance given the pathological interplay between Aβ and tau in AD [15]. When hyperphosphorylated, tau loses its affinity for microtubules and tends to aggregate forming insoluble neurofibrillary tangles, thereby causing impairment of axonal transport and synaptic functions, in addition to neurotoxicity [14]. Furthermore, pathological tau species can themselves promote the generation and neurotoxicity of Aβ oligomers and contribute to the positive feedback loop of neurodegeneration that is central to the progression of AD [69]. Our findings that fosgo-AM can attenuate Aβ-mediated generation of hyperphosphorylated tau may therefore have significant implications for the potential of fosgonimeton to impact disease progression.

Another contributor to pathological protein accumulation in AD is impairments in autophagy, which is the main mechanism by which neurons degrade and clear insoluble protein aggregates [53–55]. Components of the autophagy pathway, namely Atg5, Beclin, and ULK1, have been shown to be involved in the degradation of both Aβ and pTau [70]. Importantly, levels of Beclin-1, a core protein involved in the induction of autophagy, are downregulated in the brains of people with AD [71,72]. Preclinical studies have also demonstrated that blocking autophagic flux decreases tau clearance [73], and mice lacking key enzymes involved in autophagosome formation exhibit significant exacerbation of tau phosphorylation [74]. While the exact mechanisms remain elusive, a vicious

cycle has been proposed suggesting that accumulation of protein aggregates may overwhelm autophagic machinery, thereby blocking autophagic flux and the subsequent clearance of protein aggregates [53,75]. In our study, following $A\beta_{1-42}$ injury in primary rat cortical neurons, we noted a significant decrease in the expression of ULK1 and Beclin-1, suggesting that Aβ interfered with mechanisms governing the induction of autophagy. These deficits, however, were rectified in the presence of fosgo-AM. Given the critical roles of ULK1 and Beclin-1 in stimulating autophagy [56,76], these data provide early evidence that fosgonimeton may address autophagic impairment associated with Aβ pathology. However, this mechanistic aspect is not fully understood, and additional experiments are required to assess whether such an effect translates to an increase in autophagic flux and improved clearance of toxic proteins.

To assess whether the in vitro effects of fosgo-AM reported here translate to functional improvements in vivo, we selected an established rat model in which Aβ pathology was central to the development of cognitive impairment. ICV injection of $A\beta_{25-35}$ has been shown to recapitulate several pathological alterations of AD including short and long-term memory impairments, mitochondrial and oxidative stress, tau phosphorylation, cholinergic neuron loss, and reduced growth factors such as BDNF [60]. In our study, a single ICV administration of $A\beta_{25-35}$ induced significant cognitive impairment in the passive avoidance test 15 days later. Treatment with fosgonimeton for 14 days prior to cognitive behavioral assessment significantly restored cognitive function at all doses tested. A decreasing trend in efficacy at higher doses was observed, an effect that may be explained by negative feedback regulation inherent to growth factor systems [77–80]. Although not explored in this preliminary work, there are multiple potential points of intersection between the pathology featured in this in vivo model, and the proposed mechanism of action of fosgonimeton characterized in vitro. Neuroinflammation [81], tau phosphorylation [81,82], deficits in neurogenesis [83] and overt neuron loss [84], mitochondrial dysfunction [60], and oxidative stress [85] are a few of the reported outcomes of ICV injection of $A\beta_{25-35}$ in rodents. In our present and previous work, we have demonstrated that fosgonimeton confers some level of protection against all of these in in vitro settings. However, further studies are required to gain insight into which pathological aspects of the in vivo ICV- $A\beta_{25-35}$ model may be specifically impacted by fosgonimeton, and whether this mirrors the mechanisms observed in vitro.

Although we have previously shown that fosgo-AM potentiates HGF-mediated phosphorylation of MET in vitro and effectively distributes to the brain [40], a potential limitation in this study is the lack of data demonstrating in vivo target engagement. In this regard, additional work is required to overcome the temporal challenge of measuring the transient phospho-activation of the MET receptor in relevant brain regions. Furthermore, additional experiments are needed to elucidate the molecular mechanism by which fosgo-AM binds to the HGF/MET complex to positively modulate its activity. Such efforts have been slowed by the lack of data surrounding the crystal structure of the HGF/MET complex, as well as the overall complexity of HGF-mediated MET activation [86]. Despite these limitations, the current body of work significantly extends our understanding of a potential therapeutic role for positive modulation of neurotrophic HGF signaling in neurodegenerative disease.

Overall, this study illustrates multiple potential points for the small molecule fosgonimeton to disrupt the neurodegenerative cascade of AD downstream of Aβ toxicity, ranging from reducing oxidative stress and excitotoxicity, to improving autophagic pathway function and reducing tau hyperphosphorylation. While the recently approved Aβ-targeting monoclonal antibodies have addressed an unmet need, they are only applicable for a subset of the AD population (early AD) and the magnitude by which these therapeutics lead to a clinically meaningful benefit is limited [25,26]. Thus, additional interventions that tackle the multifactorial pathologies of AD are needed, especially for the more advanced stages of the disease (mild-to-moderate AD), where the pathological burden may be too significant to overcome via Aβ removal. Indeed, there is a growing recognition that pleiotropic approaches that address the complex pathology of AD may significantly improve treatment outcomes [87]. By positively modulating the neurotrophic HGF system, fosgonimeton represents a novel approach with a distinct MOA that can target many of the cellular dysfunctions associated with AD. Fosgonimeton (previously ATH-1017) is currently under clinical investigation for safety and efficacy in the treatment of mild-to-moderate AD (NCT04488419).

Funding

This study was designed and funded by Athira Pharma, Inc.

Author Contributions

SR: Conceptualization, Data curation, Formal analysis, Project administration, Visualization, Writing – original draft, Writing – review & editing. SS: Conceptualization, Data curation, Formal analysis, Project administration, Visualization, Writing – original draft, Writing – review & editing. A-AB: Conceptualization, Data curation, Formal analysis, Project administration, Visualization, Writing – original draft, Writing – review & editing. WW: Conceptualization, Data curation, Writing – review & editing. RT: Conceptualization, Project administration, Supervision, Writing – review & editing. JJ: Conceptualization, Project administration, Supervision, Writing – review & editing. LS: Writing – review & editing. HM: Writing – review & editing. KC: Conceptualization, Supervision, Writing – review & editing.

Declaration of competing interest

The authors declare the following financial interests/personal relationships which may be considered as potential competing interests: Kevin J Church reports a relationship with Athira Pharma Inc that includes: employment, equity or stocks, and travel reimbursement. Sherif M Reda reports a relationship with Athira Pharma Inc that includes: employment, equity or stocks, and travel reimbursement. Sharay E Setti reports a relationship with Athira Pharma Inc that includes: employment, equity or stocks, and travel reimbursement. Andree-Anne Berthiaume reports a relationship with Athira Pharma Inc that includes: employment, equity or stocks, and travel reimbursement. Wei Wu reports a relationship with Athira Pharma Inc that includes: employment, equity or stocks, and travel reimbursement. Robert W Taylor reports a relationship with Athira Pharma Inc that includes: employment, equity or stocks, and travel reimbursement. Jewel L Johnston reports a relationship with Athira Pharma Inc that includes: employment, equity or stocks, and travel reimbursement. Liana R Stein reports a relationship with Athira Pharma Inc that includes: employment, equity or stocks, and travel reimbursement. Hans J Moebius reports a relationship with Athira Pharma Inc that includes: employment, equity or stocks, and travel reimbursement. Kevin J Church has patent issued to Athira Pharma Inc. If there are other authors, they declare that they have no known competing financial interests or personal relationships that could have appeared to influence the work reported in this paper.

Acknowledgements

The authors thank Neuro-Sys, SAS and Neurofit, SAS for their execution and data collection of the in vitro and in vivo experiments, respectively, which were funded by Athira Pharma, Inc. We appreciate the assistance of Noëlle Callizot and Alexandre Henriques (Neuro-Sys, SAS) in revising the manuscript and ensuring the accurate depiction and interpretation of the data.

Appendix A. Supplementary data

Supplementary data to this article can be found online at https://doi.org/10.1016/j.neurot.2024.e00350.

References

[1] 2022 Alzheimer's disease facts and figures. Alzheimers Dement 2022 Apr 1;18(4):700–89.
[2] Chen JX, Yan SD. Amyloid- -induced mitochondrial dysfunction. J Alzheim Dis 2007;12(2):177–84.
[3] Wang R, Reddy PH. Role of glutamate and NMDA receptors in Alzheimer's disease. J Alzheim Dis 2016 Sep 23;57(4):1041–8.
[4] Gate. Neuroinflammation in Alzheimer's disease. J Neurol Sci 2021 Oct 1;429.
[5] Heneka MT, Carson MJ, Khoury JE, Landreth GE, Brosseron F, Feinstein DL, et al. Neuroinflammation in Alzheimer's disease. Lancet Neurol 2015 Apr 1;14(4):388–405.
[6] Peña-Bautista C, Torres-Cuevas I, Baquero M, Ferrer I, García L, Vento M, et al. Early neurotransmission impairment in non-invasive Alzheimer Disease detection. Sci Rep 2020 Dec 1;10(1).
[7] Kaur S, DasGupta G, Singh S. Altered neurochemistry in Alzheimer's disease: targeting neurotransmitter receptor mechanisms and therapeutic strategy. Neurophysiology 2019 Jul 1;51(4):293–309.
[8] Schindowski K, Belarbi K, Buée L. Neurotrophic factors in Alzheimer's disease: role of axonal transport. Gene Brain Behav 2008 Jan 3;7:43–56.
[9] Allen S J, Watson J J, Dawbarn D. The neurotrophins and their role in alzheimers disease. Curr Neuropharmacol 2011 Dec 1;9(4):559–73.
[10] Cai Huan, Cong Wei-na, Ji Sunggoan, Rothman Sarah, Maudsley Stuart, Martin Bronwen. Metabolic dysfunction in alzheimers disease and related neurodegenerative disorders. Curr Alzheimer Res 2012 Jan 1;9(1):5–17.
[11] Gu X-M, Huang H-C, Jiang Z-F. Mitochondrial dysfunction and cellular metabolic deficiency in Alzheimer's disease. Neurosci Bull 2012 Oct 1;28(5):631–40.
[12] Iadecola C, Gottesman RF. Cerebrovascular alterations in alzheimer disease. Circ Res 2018 Aug 3;123(4):406–8.
[13] Selkoe DJ, Hardy J. The amyloid hypothesis of Alzheimer's disease at 25 years. EMBO Mol Med 2016 Jun 1;8(6):595–608.
[14] Mucke L, Selkoe DJ. Neurotoxicity of amyloid β-protein: synaptic and network dysfunction. Cold Spring Harb Perspect Med. 2012 Jul 1;2(7):A6338.
[15] Guo T, Zhang D, Zeng Y, Huang TY, Xu H, Zhao Y. Molecular and cellular mechanisms underlying the pathogenesis of Alzheimer's disease. Mol Neurodegener 2020 Dec 1;15(1).
[16] Carrillo-Mora P, Luna R, Colín-Barenque L, Pedraza-Chaverri J. Amyloid beta: multiple mechanisms of toxicity and only some protective effects? Oxid Med Cell Longev 2014 Feb;5:2014.
[17] Keil U, Steiner B, Haass C, Müller W, Eckert A. Amyloid beta induces mitochondrial dysfunction in a dose-dependent manner. Pharmacopsychiatry 2004 Jun 9;36(5).
[18] Abramov AY, Canevari L, Duchen MR. β-Amyloid peptides induce mitochondrial dysfunction and oxidative stress in astrocytes and death of neurons through activation of NADPH oxidase. J Neurosci 2004 Jan 14;24(2):565–75.
[19] Callizot N, Combes M, Steinschneider R, Poindron P. Operational dissection of β-amyloid cytopathic effects on cultured neurons. J Neurosci Res 2013 Mar 8;91(5):706–16.
[20] de la Cueva M, Antequera D, Ordoñez-Gutierrez L, Wandosell F, Camins A, Carro E, et al. Amyloid-β impairs mitochondrial dynamics and autophagy in Alzheimer's disease experimental models. Sci Rep 2022 Jun 16;12.
[21] Zhang W, Xu C, Sun J, Shen H-M, Wang J, Yang C. Impairment of the autophagy–lysosomal pathway in Alzheimer's diseases: pathogenic mechanisms and therapeutic potential. Acta Pharm Sin B 2022 Mar 1;12(3):1019–40.
[22] Magrane J, Rosen KM, Smith RC, Walsh K, Gouras GK, Querfurth HW. Intraneuronal -amyloid expression downregulates the akt survival pathway and blunts the stress response. J Neurosci 2005 Nov 23;25(47):10960–9.
[23] Zhang F, Gannon M, Chen Y, Yan S, Zhang S, Feng W, et al. β-amyloid redirects norepinephrine signaling to activate the pathogenic GSK3β/tau cascade. Sci Transl Med 2020 Jan 15;12(526):EAAY6931.
[24] Lee H-K, Kumar P, Fu Q, Rosen KM, Querfurth HW. The insulin/akt signaling pathway is targeted by intracellular -amyloid. Mol Biol Cell 2009 Mar 1;20(5):1533–44.
[25] Lecanemab in early Alzheimer's disease. N Engl J Med 2023 Apr 27;388(17):1630–2.
[26] Petersen RC, Aisen PS, Andrews JS, Atri A, Matthews BR, Rentz DM, et al. Expectations and clinical meaningfulness of randomized controlled trials. Alzheimers Dement 2023 Jun 1;19(6):2730–6.
[27] Haass C, Selkoe D. If amyloid drives Alzheimer disease, why have anti-amyloid therapies not yet slowed cognitive decline? PLoS Biol 2022 Jul 1;20(7).
[28] Moebius HJ, Church KJ. The case for a novel therapeutic approach to dementia: small molecule hepatocyte growth factor (HGF/MET) positive modulators. J Alzheim Dis 2023 Mar 7;92(1):1–12.
[29] Mitra S, Behbahani H, Eriksdotter M. Innovative therapy for Alzheimer's disease-with focus on biodelivery of NGF. Front Neurosci 2019;13:38.
[30] Nasrolahi A, Javaherforooshzadeh F, Jafarzadeh-Gharehziaaddin M, Mahmoudi J, Asl KD, Shabani Z. Therapeutic potential of neurotrophic factors in Alzheimer's Disease. Mol Biol Rep 2022 Mar 1;49(3):2345–57.
[31] Jiao S-S, Shen L-L, Zhu C, Bu X-L, Liu Y-H, Liu C-H, et al. Brain-derived neurotrophic factor protects against tau-related neurodegeneration of Alzheimer's disease. Transl Psychiatry 2016 Oct 4;6(10):E907.
[32] Funakoshi H, Nakamura T. Hepatocyte growth factor (HGF): neurotrophic functions and therapeutic implications for neuronal injury/diseases. Curr Signal Transduct Ther 2011 May 1;6(2):156–67.
[33] Desole C, Gallo S, Vitacolonna A, Montarolo F, Bertolotto A, Vivien D, et al. HGF and MET: from brain development to neurological disorders. Front Cell Dev Biol 2021;9:683609.
[34] Matsumoto K, Funakoshi H, Takahashi H, Sakai K. HGF-met pathway in regeneration and drug discovery. Biomedicines 2014 Oct 31;2(4):275–300.
[35] Machide M, Kamitori K, Nakamura Y, Kohsaka S. Selective activation of phospholipase C gamma1 and distinct protein kinase C subspecies in intracellular signaling by hepatocyte growth factor/scatter factor in primary cultured rat neocortical cells. J Neurochem 1998 Aug 1;71(2):592–602.
[36] Xiao G-H, Jeffers M, Bellacosa A, Mitsuuchi Y, Vande Woude GF, Testa JR. Anti-apoptotic signaling by hepatocyte growth factor/Met via the phosphatidylinositol 3-kinase/Akt and mitogen-activated protein kinase pathways. Proc Natl Acad Sci U S A 2001 Jan 2;98(1):247–52.
[37] Akimoto M, Baba A, Ikeda-Matsuo Y, Yamada MK, Itamura R, Nishiyama N, et al. Hepatocyte growth factor as an enhancer of nmda currents and synaptic plasticity in the hippocampus. Neuroscience 2004;128(1):155–62.
[38] Hamasaki H, Honda H, Suzuki SO, Hokama M, Kiyohara Y, Nakabeppu Y, et al. Down-regulation of MET in hippocampal neurons of Alzheimer's disease brains. Neuropathology 2014 Jun 2;34(3):284–90.
[39] Wei J, Ma X, Nehme A, Cui Y, Zhang L, Qiu S. Reduced HGF/MET signaling may contribute to the synaptic pathology in an Alzheimer's disease mouse model. Front Aging Neurosci 2022 Jul 12;14.
[40] Johnston JL, Reda SM, Setti SE, Taylor RW, Berthiaume A-A, Walker WE, et al. Fosgonimeton, a novel positive modulator of the HGF/MET system, promotes neurotrophic and procognitive effects in models of dementia. Neurotherapeutics 2023 Mar 1;20(2):431–51.
[41] Han X-J, Hu Y-Y, Yang Z-J, Jiang L-P, Shi S-L, Li Y-R, et al. Amyloid β-42 induces neuronal apoptosis by targeting mitochondria. Mol Med Rep 2017 Oct 1;16(4):4521–8.
[42] Wang W, Zhao F, Ma X, Perry G, Zhu X. Mitochondria dysfunction in the pathogenesis of Alzheimer's disease: recent advances. Mol Neurodegener 2020 May 29;15(1):30.
[43] Moreira PI, Carvalho C, Zhu X, Smith MA, Perry G. Mitochondrial dysfunction is a trigger of Alzheimer's disease pathophysiology. Biochim Biophys Acta, Mol Basis Dis 2010 Jan 1;1802(1):2–10.
[44] Vauzour D, Vafeiadou K, Rice-Evans C, Williams RJ, Spencer JPE. Activation of pro-survival Akt and ERK1/2 signalling pathways underlie the anti-apoptotic effects of flavanones in cortical neurons. J Neurochem 2007 Jul 17;103(4):1355–67.
[45] Kennedy SG, Kandel ES, Cross TK, Hay N. Akt/protein kinase B inhibits cell death by preventing the release of cytochrome c from mitochondria. Mol Cell Biol 1999 Aug 1;19(8):5800–10.
[46] Long H-Z, Cheng Y, Zhou Z-W, Luo H-Y, Wen D-D, Gao L-C. PI3K/AKT signal pathway: a target of natural products in the prevention and treatment of Alzheimer's disease and Parkinson's disease. Front Pharmacol 2021;12:648636.
[47] Karmarkar SW, Bottum KM, Krager SL, Tischkau SA. ERK/MAPK is essential for endogenous neuroprotection in SCN2.2 cells. PLoS One 2011;6(8):E23493.
[48] Silingardi D, Angelucci A, De Pasquale R, Borsotti M, Squitieri G, Brambilla R, et al. ERK pathway activation bidirectionally affects visual recognition memory and synaptic plasticity in the perirhinal cortex. Front Behav Neurosci 2011;5:84.
[49] Peng S, Zhang Y, Zhang J, Wang H, Ren B. ERK in learning and memory: a review of recent research. Int J Mol Sci 2010 Jan 13;11(1):222–32.
[50] Teich A, Nicholls R, Puzzo D, Fiorito J, Purgatorio R, Fa' M, et al. Synaptic therapy in Alzheimer's disease: a CREB-centric approach. Neurotherapeutics 2015 Jan 1;12(1):29–41.
[51] Zhang H, Wei W, Zhao M, Ma L, Jiang X, Pei H, et al. Interaction between Aβ and tau in the pathogenesis of Alzheimer's disease. Int J Biol Sci 2021;17(9):2181–92.
[52] Sayas CL, Ávila J. GSK-3 and tau: a key duet in Alzheimer's disease. Cells 2021 Mar 24;10(4).
[53] Uddin MS, Stachowiak A, Mamun AA, Tzvetkov NT, Takeda S, Atanasov AG, et al. Autophagy and Alzheimer's disease: from molecular mechanisms to therapeutic implications. Front Aging Neurosci 2018;10:4.
[54] Stavoe AKH, Holzbaur ELF. Autophagy in neurons. Annu Rev Cell Dev Biol 2019 Oct 6;35(1):477–500.
[55] Zhang Yang, Song Tu. Autophagy in Alzheimer's disease pathogenesis: therapeutic potential and future perspectives. Ageing Res Rev 2021 Dec 1:72.
[56] Menon MB, Dhamija S. Beclin 1 phosphorylation - at the center of autophagy regulation. Front Cell Dev Biol 2018;6:137.
[57] Park J-M, Seo M, Jung CH, Grunwald D, Stone M, Otto NM, et al. ULK1 phosphorylates Ser30 of BECN1 in association with ATG14 to stimulate autophagy induction. Autophagy 2018 Apr 3;14(4):584–97.
[58] Russell Ryan C, Ye Tian, Yuan Haixin, Park Hyun Woo, Yu-Yun Chang, Kim Joungmok, et al. ULK1 induces autophagy by phosphorylating Beclin-1 and activating VPS34 lipid kinase. Nat Cell Biol 2013 Jul 1;15(7):741–50.
[59] Hampel H, Hardy J, Blennow K, Chen C, Perry G, Kim SH, et al. The amyloid-β pathway in Alzheimer's disease. Mol Psychiatr 2021 Oct 1;26(10):5481–503.
[60] Zussy C. Alzheimer's disease related markers, cellular toxicity and behavioral deficits induced six weeks after oligomeric amyloid-beta peptide injection in rats. PLoS One 2013 Jan 2;8(1):636–55.
[61] Bayer TA, Wirths O. Intracellular accumulation of amyloid-Beta - a predictor for synaptic dysfunction and neuron loss in Alzheimer's disease. Front Aging Neurosci 2010;2:8.
[62] Naldi M, Fiori J, Pistolozzi M, Drake AF, Bertucci C, Wu R, et al. Amyloid β-peptide 25–35 self-assembly and its inhibition: a model undecapeptide system to gain atomistic and secondary structure details of the Alzheimer's disease process and treatment. ACS Chem Neurosci 2012 Nov 21;3(11):952–62.
[63] Pugazhenthi S, Nesterova A, Sable C, Heidenreich KA, Boxer LM, Heasley LE, et al. Akt/protein kinase B up-regulates bcl-2 expression through cAMP-response element-binding protein*. J Biol Chem 2000 Apr 14;275(15):10761–6.

[64] Ying JIN, En-zhi YAN, Ying FAN, Xiao-li GUO, Yan-jie ZHAO, Zhi-hong ZONG, et al. Neuroprotection by sodium ferulate against glutamate-induced apoptosis is mediated by ERK and PI3 kinase pathways 1. Acta Pharmacol Sin 2007;28(12): 1881–90.
[65] Almeida RD, Manadas BJ, Melo CV, Gomes JR, Mendes CS, Grãos MM, et al. Neuroprotection by BDNF against glutamate-induced apoptotic cell death is mediated by ERK and PI3-kinase pathways. Cell Death Differ 2005 Oct 1;12(10): 1329–43.
[66] Asomugha CO, Linn DM, Linn CL. ACh receptors link two signaling pathways to neuroprotection against glutamate-induced excitotoxicity in isolated RGCs. J Neurochem 2009 Dec 8;112(1):214–26.
[67] Danysz W, Parsons CG. Alzheimer's disease, β-amyloid, glutamate, NMDA receptors and memantine – searching for the connections. Br J Pharmacol 2012 Aug 22; 167(2):324–52.
[68] Revett Timothy, Baker G, Jhamandas J, Kar S. Glutamate system, amyloid β peptides and tau protein: functional interrelationships and relevance to Alzheimer disease pathology. J Psychiatr Neurosci : JPN 2013 Jan 1;38(1):6–23.
[69] Bloom GS. Amyloid-β and tau: the trigger and bullet in Alzheimer disease pathogenesis. JAMA Neurol 2014 Apr 1;71(4):505–8.
[70] Tian Y, Bustos V, Flajolet M, Greengard P. A small-molecule enhancer of autophagy decreases levels of A and APP-CTF via Atg5-dependent autophagy pathway. Faseb J 2011 Jun 1;25(6):1934–42.
[71] Pickford F, Masliah E, Britschgi M, Lucin K, Narasimhan R, Jaeger PA, et al. The autophagy-related protein beclin 1 shows reduced expression in early Alzheimer disease and regulates amyloid beta accumulation in mice. J Clin Invest 2008 Jun 1; 118(6):2190–9.
[72] Rohn TT, Wirawan E, Brown RJ, Harris JR, Masliah E, Vandenabeele P. Depletion of Beclin-1 due to proteolytic cleavage by caspases in the Alzheimer's disease brain. Neurobiol Dis 2011 Jul 1;43(1):68–78.
[73] Hamano T, Gendron TF, Causevic E, Yen S, Lin W, Isidoro C, et al. Autophagic-lysosomal perturbation enhances tau aggregation in transfectants with induced wild-type tau expression. Eur J Neurosci 2008 Mar 19;27(5):1119–30.
[74] Inoue K, Rispoli J, Kaphzan H, Klann E, Chen EI, Kim J, et al. Macroautophagy deficiency mediates age-dependent neurodegeneration through a phospho-tau pathway. Mol Neurodegener 2012 Dec 1;7(1).
[75] Chen J, He H-J, Ye Q, Feng F, Wang W-W, Gu Y, et al. Defective autophagy and mitophagy in Alzheimer's disease: mechanisms and translational implications. Mol Neurobiol 2021 Oct 1;58(10):5289–302.
[76] Lane JD, Korolchuk VI, Murray JT, Zachari M, Ganley IG. The mammalian ULK1 complex and autophagy initiation. Essays Biochem 2017 Dec 12;61(6):585–96.
[77] Mattson MP. Hormesis defined. Ageing Res Rev 2008 Jan 1;7(1):1–7.
[78] Calabrese EJ, Baldwin LA. Defining hormesis. Hum Exp Toxicol 2002 Feb 1;21(2): 91–7.
[79] Roi Avraham, Yosef Yarden. Feedback regulation of EGFR signalling: decision making by early and delayed loops. Nat Rev Mol Cell Biol 2011 Feb 1;12(2): 104–17.
[80] Chandarlapaty S, Sawai A, Scaltriti M, Rodrik-Outmezguine V, Grbovic-Huezo O, Serra V, et al. AKT inhibition relieves feedback suppression of receptor tyrosine kinase expression and activity. Cancer Cell 2011 Jan 18;19(1):58–71.
[81] Kuang X, Du JR, Chen YS, Wang J, Wang YN. Protective effect of Z-ligustilide against amyloid @b-induced neurotoxicity is associated with decreased pro-inflammatory markers in rat brains. Pharmacol Biochem Behav 2009 Jun 1;92(4): 635–41.
[82] Park SH, Kim JH, Bae SS, Hong KW, Lee DS, Leem JY, et al. Protective effect of the phosphodiesterase III inhibitor cilostazol on amyloid @b-induced cognitive deficits associated with decreased amyloid @b accumulation. Biochem Biophys Res Commun 2011 May 20;408(4):602–8.
[83] Kim B-K, Shin M-S, Kim C-J, Baek S-B, Ko Y-C, Kim Y-P. Treadmill exercise improves short-term memory by enhancing neurogenesis in amyloid beta-induced Alzheimer disease rats. J Exerc Rehabil 2014 Feb 1;10(1):2–8.
[84] Stepanichev MY, Zdobnova IM, Zarubenko II, Moiseeva YV, Lazareva NA, Onufriev MV, et al. Amyloid-@b(25-35)-induced memory impairments correlate with cell loss in rat hippocampus. Physiol Behav 2004 Feb 1;80(5):647–55.
[85] Lu P, Mamiya T, Lu L, Mouri A, Ikejima T, Kim H-C, et al. Xanthoceraside attenuates amyloid ß peptide25–35-induced learning and memory impairments in mice. Psychopharmacology (Berl) 2012 Jan 1;219(1):181–90.
[86] Uchikawa E, Chen Z, Xiao G-Y, Zhang X, Bai X. Structural basis of the activation of c-MET receptor. Nat Commun 2021 Jul 1;12(1).
[87] Ju Y, Tam K. Pathological mechanisms and therapeutic strategies for Alzheimer's disease. Neural Regen Res 2022 Mar 1;17(3):543–9.